PART III

IMAGING OF VESSEL WALL MORPHOLOGY AND FUNCTION

CHAPTER 8

COUPLING OF VESSEL WALL MORPHOLOGY AND FUNCTION IN THE AORTA AND THE CAROTID ARTERY: AN EVALUATION WITH MRI

E.S.J. Kröner, H.J. Lamb, H.J. Siebelink, H. Putter, R.J. van der Geest, E.E. van der Wall, A. de Roos, J.J.M. Westenberg

Int J Cardiovasc Imaging 2014;30:91-8.

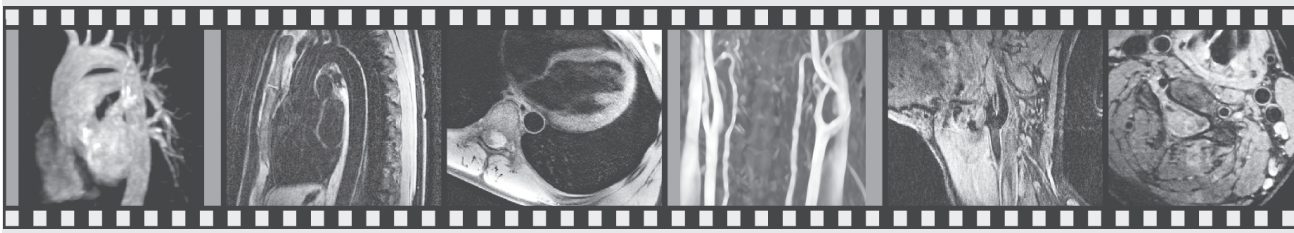

ABSTRACT

Purpose:o evaluate the regional association between vessel wall morphology (i.e. cross-sectional vessel wall area (VWA)) and function (i.e. wall stiffness expressed in the pulse wave velocity (PWV)) in both the aortic arch and the left carotid artery.

Methods: Thirty-two healthy volunteers (mean age 41 ±16 years) underwent 3T MRI examination to assess PWV and VWA of the aorta and the left carotid artery. PWV was determined by the transit-time method with velocity-encoded MRI recordings of the systolic blood flow propagation. VWA was assessed for both the aorta and the carotid artery, by detecting lumen and outer vessel wall contours in cross-sectional black blood images. Linear regression analyses were used to test associations between aortic and carotid vessel wall area and stiffness.

Results: Within the same vascular territory, correlation between PWV and VWA was stronger than across vascular territories. For the aorta, the correlation between PWV_{AO} and VWA_{AO} ($r=0.71$, $p<0.0001$) was stronger than between PWV_{AO} and VWA_{CA} ($r=0.53$, $p=0.002$). For the carotid artery, the correlation between PWV_{CA} and VWA_{CA} ($r=0.61$, $p<0.0001$) was stronger than between PWV_{CA} and VWA_{AO} ($r=0.46$, $p=0.008$).

Conclusion: Morphologic and functional vessel wall properties assessed in the aortic arch and the left carotid artery are significantly stronger associated within the same vascular territory rather than across different vascular territories.

INTRODUCTION

Abnormal arterial stiffening and vessel wall thickening have proven to be associated with major cardiovascular disease end points, including heart disease and stroke (1). Therefore, arterial stiffness and cross-sectional vessel wall area (VWA) are commonly assessed to evaluate cardiovascular risk (2).

Aging interacting with various environmental factors exerts effect on both the morphology and function of the arterial vessel wall by media degeneration and breakdown of elastic fibers (3), eventually leading to an increased stiffness of the arterial vessel wall. Using echo Doppler, a different effect of age on arterial stiffening in the aortic arch as compared to the common carotid artery has been demonstrated (4).

In young healthy subjects, a portion of the systolic pressure waves is thought be reflected due to the stiffness mismatch at the interface between the compliant aorta and the stiffer carotid arteries (5). Recently it was suggested that abnormal stiffening of the aorta may result in the loss of the protective effect of the stiffness mismatch, allowing excessive pulsatile energy transmitted from the aorta to the brain which might be a factor in the occurrence of cerebrovascular lesions (4,6).

Using magnetic resonance imaging (MRI) in combination with velocity-encoding (VE), non-invasive evaluation of both morphological (such as VWA) and functional vessel wall parameters (such as wall stiffness expressed in the pulse wave velocity (PWV)) is feasible in arbitrarily chosen vascular territories (1,7-10). PWV, defined as the propagation speed of the systolic pressure wave front through the aorta, is a proven and clinically useful surrogate marker of arterial stiffness (1). PWV assessment by MRI is a well-validated method to non-invasively quantify arterial stiffness (1,9,11). In contrast to echocardiography, MRI allows for a regional assessment of PWV, as MRI is not limited to the availability of suitable acoustic windows along the vascular tree.

We hypothesize that the association between PWV and VWA is regionally different between vascular beds and territories. Differential stiffening in various vascular territories may cause site-specific perfusion abnormalities supplying various organs such as the brain, the heart, the kidneys and alike. Accordingly, the purpose of this study was to assess the relationship between PWV and VWA in two vascular territories (i.e., the aortic arch and the left carotid artery, respectively) and across both territories.

MATERIAL AND METHODS

Population and study protocol

Thirty-two healthy asymptomatic volunteers without history of cardiovascular disease, stroke, transient ischemic attack or dementia and without cardiovascular medication were included. The characteristics of the study population are summarized in Table 1. Mean systolic blood pressure was 124 ±12 mmHg and mean diastolic blood pressure 75 ± 8 mmHg. Mean heart rate was 62 ± 9 beats/minute and all volunteers were in

regular sinus rhythm. Fifteen volunteers (47%) were male. Mean BMI was 23.0 ± 2.2 kg/m^2. Approval from the local medical ethics committee was obtained and all subjects gave written informed consent. Part of the data of this study group has been published before in a study focusing on age-relation and PWV leveling.

Subjects underwent 3T MRI examination (Achieva, Philips Medical Systems, Best, The Netherlands) between August 2011 and March 2012 to assess PWV in the aortic arch and the carotid artery and measurements for aorta and carotid artery vessel wall area (VWA) using validated MRI techniques. The relation between functional (PWV_{AO} in the aorta and PWV_{CA} in the carotid artery) and morphologic measures (VWA_{AO} in the aorta and VWA_{CA} in the carotid artery) within the same vascular territory and across vascular territories was assessed.

Table 1: Characteristics of study population (n=32)

Male/Female	15/17
Age (years)	41 ± 16 (range: 20 – 68 years)
Systolic blood pressure (mmHg)	124 ± 12
Diastolic blood pressure (mmHg)	75 ± 8
Heart rate (beats/minute)	62 ± 9
BMI (kg/m^2)	23 ± 2
BSA (m^2)	1.9 ± 0.2
Aortic flow volume per minute/BSA (ml/min/m^2)	2936 ± 724

Data are represented as mean ± standard deviation or median (range).
Abbreviations: BMI: body mass index, BSA: body surface area.

MRI Acquisition

Aortic and carotid arterial pulse wave velocity

Using a dedicated cardiac coil (6-element phased-array coil), PWV_{AO} was assessed by means of one through-plane VE MRI acquisition perpendicular to the aorta, at the level of the pulmonary artery, transecting both the ascending and proximal descending aorta (Figure 1 A1) to assess the blood flow velocity (Figure 1 A2) (12).

Scan parameters VE MRI acquisition: field-of-view (FOV) 320×260 mm^2, slice thickness 8 mm, flip angle (FA) 10°, repetition time (TR) 4.9 ms, echo time (TE) 2.9 ms, acquisition resolution 2.5×2.5×8.0 mm^3, number of signal averages (NSA) 1, velocity sensitivity (V_{enc}) 150 cm/s in through-plane direction. The true maximal temporal resolution (TRes, defined as 2×TR) amounted to 9.8 ms. Vector ECG-triggering with retrospective gating was used with maximal number of phases reconstructed. Scan duration depended on the subject's heart rate and was approximately 2 minutes at 60 beats per minute heart rate.

Using a 16-element neurovascular head-neck coil, PWV in the carotid artery (PWV_{CA}) was assessed by means of two consecutive through-plane VE MRI acquisitions, planned perpendicular to the left carotid artery using a rotational maximal-intensity-projection (MIP) of a three-dimensional (3D) time-of-flight registration of the carotid circulation,

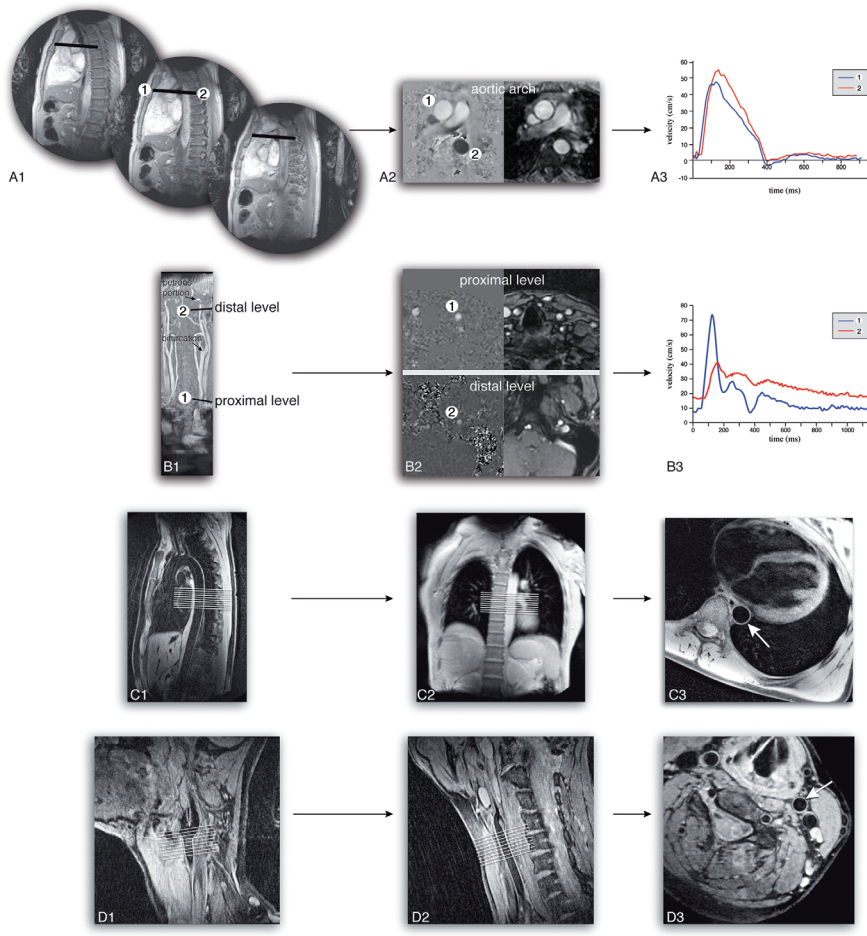

Figure 1. Representation of methods for pulse wave velocity and vessel wall area assessment, both for the aorta (AO) and the carotid artery (CA)**.** (**A**) PWV_{AO} was assessed by means of one through-plane velocity-encoded MRI acquisition, planned at the level of the pulmonary trunk, transecting both the ascending aorta (1) and proximal descending aorta (2) (**A1**), resulting in the following velocity-encoded images (**A2**)**.** From the propagation of the velocity-time waveforms (**A3**), PWV_{AO} is determined.
(**B**) PWV_{CA} was assessed by means of two-slice through-plane velocity-encoded MRI at two locations, proximally at the left common carotid artery just above the aortic arch (1) and distally just below the petrous portion of the left internal carotid artery (2) (**B1**), which were planned on the rotational maximum-intensity-projection of a 3D Time-Of-Flight acquisition of the carotid arteries. The velocity-encoded images acquired in the carotid artery are represented in **(B2).** From the propagation of the velocity waveforms (**B3**), PWV_{CA} is determined.
(**C**) VWA_{AO} was determined with a 2 cm thick 3-dimensional volume acquisition (in white) consisting of 10 slices positioned on two aortic survey scans; a double-oblique sagittal black-blood image of the aorta (**C1**) and double-oblique coronal bright-blood image of the aorta (**C2**). From the resulting cross-sectional black-blood images of the aorta (**C3,** aorta is indicated by white arrow), VWA_{AO} is determined.
(D) VWA_{CA} was determined with a 1.6 cm multi-slice 2-dimensional acquisition stack (in white) consisting of 9 slices positioned on two carotid artery survey scans; a double-oblique sagittal black-blood image of the carotid artery **(D1)** and a double-oblique coronal image of the carotid artery **(D2)**. From the resulting cross-sectional black-blood images of the carotid artery **(D3,** carotid artery is indicated by white arrow**),** VWA_{CA} is determined.

to assess the blood flow velocity (Figure 1 B1,2). The first acquisition was positioned proximally at the origin of the common carotid artery, just above the aortic arch and the second acquisition was positioned distal to the bifurcation and just below the petrous portion of the internal carotid artery (Figure 1 B1).

Scan parameters 3D TOF: T1-weighted gradient-echo, FOV 180×172 mm^2, 350 over-contiguous slices, slice thickness 2 mm, TR 23 ms, TE 3.45 ms, FA 15°, acquisition resolution: 1.0×2.8×2.0 mm^3.

Scan parameters VE acquisitions: FOV 200×200 mm^2 , slice thickness 5 mm, FA 10°, TR 6.2 ms, TE 3.4 ms, acquisition resolution 1.52×1.50×5.0 mm^3, NSA 1, V_{enc} was 150 cm/s for first acquisition at the common carotid artery and V_{enc} was 120 cm/s for the second acquisition at the internal carotid artery, with velocity encoding both in through-plane direction. TRes amounted to 12.4 ms. Vector ECG-triggering with retrospective gating was used with the maximal number of phases reconstructed. Scan duration depended on the subject's heart rate and was approximately 2 minutes for each acquisition.

Aortic and carotid vessel wall area

VWA_{AO} was determined using a standardized scan protocol, which was described before (10). Briefly, a 3D dual-inversion-recovery black-blood segmented k-space gradient-echo imaging sequence with fat suppression was planned perpendicular to both a sagittal (Figure 1 C1) and coronal view (Figure 1 C2) of the aorta and was reconstructed into 10 cross-sectional slices of 2 mm (Figure 1 C3) (13). The upper level of the 3D volume slab was positioned at the level of the upper edge of the eight thoracic vertebra. Scan parameters: FOV 270×203 mm^2, slice thickness 2 mm, FA 20°, TR 4.9 ms, TE 2.5 ms, acquisition resolution 0.53×0.53×2.0 mm^3, NSA 2. Vector ECG-triggering at end-diastole was used. Data were acquired at every other heartbeat to suppress signal of slow blood flow in the lumen. Respiratory motion suppression was achieved by navigator gating with a 5 mm gating window, positioned at the top of the hemi-diaphragm (10). Scan duration depended on heart rate and navigator efficiency and was approximately 6.5 minutes.

VWA_{CA} was determined using a standardized scan protocol, previously described in full (14). Briefly, a standard Philips SENSE-flex-M surface coil with two flexible elements of 14×17 cm was positioned around the neck. A 2D T1-weighted segmented gradient echo-sequence was planned on sagittal and coronal surveys scans (Figure 1 D1,2), perpendicular to the course of the common carotid artery in both views (Figure 1 D3). Nine contiguous transverse slices of 2 mm thickness were positioned perpendicular to the left common carotid artery, starting from the carotid bifurcation in the proximal (caudal) direction. Scan parameters: 2-dimensional (2D) black-blood T1-weighted fast gradient echo sequence, FOV 140×140 mm^2, 2.0 mm slice thickness, FA 45°, TR 12.4 ms, TE 3.5 ms, acquired resolution 0.46×0.46×2.0 mm^3, NSA 2. Vector ECG-triggering at end-diastole was used. Scan duration depended on the subject's heart rate and was approximately 10 minutes (for 9 slices at a mean heart rate of 60 beats per minutes).

Image analysis

Aortic and carotid arterial pulse wave velocity

PWV_{AO} and PWV_{CA} were both determined by the transit-time method (15). Using MASS software (Leiden University Medical Center, Leiden, The Netherlands), the distance between two sampling sites (Δx) was manually determined by placing a poly-line along the vessel centerline.

This was performed for the aorta by using the sagittal survey images and for the carotid artery by using the rotational MIP of the TOF image. Using FLOW software (Leiden University Medical Center, Leiden, The Netherlands) with automated contour detection for image segmentation, wave propagation was evaluated from maximal velocity-time curves that were obtained at all sampling sites (Figure 1 A3, B3). The foot-to-foot definition was used for Δt (i.e., the transit-time)-assessment, with automated detection of the foot of the systolic velocity wave front (i.e., the wave arrival time). Accordingly, PWV was calculated as Δx/Δt (m/s) (9).

Aortic and carotid vessel wall area

VWA analysis was performed using the VesselMass software (Leiden University Medical Center, Leiden, The Netherlands). Lumen and outer wall contours were detected as was previously described (16,17). For the aorta, contour segmentation was performed in eight slices out of ten. Both outer slices of the stack were disregarded as image quality may vary in the outer slices of a 3D image set due to band width drop-off. For the carotid artery, slices were excluded for analysis only at the distal part of the imaging stack, when the bifurcation of the carotid artery was already present in the image and possibly influencing analysis of common carotid artery vessel wall thickness. Contour segmentation was performed in at least three slices out of nine slices and a maximum of analyzed slices was six. The average vessel wall area is represented as cross-sectional area (mm^2), averaged over all included slices. Consecutively, for both the aorta and the carotid artery, vessel wall was indexed for body surface area (BSA) (in mm^2/m^2), determined according to the Mosteller's formula (18).

Statistical analysis

Continuous variables are expressed as mean ± standard deviation (SD). Univariable linear regression analyses were performed for the total study population to assess the associations between VWA and PWV. The values for VWA were not normally distributed and therefore log transformed to assess the association between VWA and PWV. Younger or older age (as binary variable) was included as an independent variable in the linear regression analyses to acquire age-adjusted regression lines. Regression lines and 95%CIs of the slope are reported. To assess the relative strength of the predictive values of VWA_{AO} and VWA_{CA} for PWV_{AO}, a forward selection model was used, with VWA_{AO} and VWA_{CA} as dependent variables and PWV_{AO} as independent variable. The predictive value of VWA_{AO} and VWA_{CA} for PWV_{CA} was similarly assessed.

RESULTS

Mean evaluated aortic arch trajectory was 115 ± 24 mm and mean evaluable left carotid artery trajectory was 174 ± 11 mm.

PWV and VWA of the aorta and carotid artery

Mean values for PWV and VWA are presented in Table 2. For the total study population, mean PWV_{AO} was not significantly different compared to mean PWV_{CA} (6.1 ± 1.7 m/s versus 6.3 ± 1.4 m/s, p=0.55).

Table 2: MRI results

Trajectory aorta (mm)	115 ± 24
Trajectory carotid artery (mm)	174 ± 11
PWV aorta (m/s)	6.1 ± 1.7
PWV carotid artery (m/s)	6.3 ± 1.4
Aorta vessel wall area/BSA (average per slice, mm^2/m^2)	47.1 (38.1 – 58)
Carotid artery vessel wall area/BSA (average per slice, mm^2/m^2)	12.7 (11.2 – 15.7)

Data are represented as mean ± standard deviation or as median (interquartile range).
Abbreviations: PWV: pulse wave velocity, BSA: body surface area.

Associations within the same vascular territory

The linear regression analyses between PWV and VWA within the same vascular territory are presented in Figure 2A,B for the aorta and carotid artery respectively. Significant correlations were observed between PWV and VWA within the same vascular territory (Table 3). For the aorta, the relation between PWV and VWA was influenced by age indicated by the reduced slope in the age-adjusted regression line. For the carotid artery, the observed association between PWV and VWA was less influenced by age.

Associations across vascular territories

The linear regression analyses between PWV and VWA across vascular territories are presented in Figure 3A,B. Across vascular territories, PWV and VWA were correlated (Table 3), but these associations were less strong when compared to the associations within vascular territories, both for the aorta (r=0.71, p<0.0001 for PWV_{AO} and VWA_{AO} versus r= 0.53, p=0.002 for PWV_{AO} and VWA_{CA}, respectively) as well as for the carotid artery (r=0.61, p<0.0001 for PWV_{CA} and VWA_{CA} versus r=0.46, p=0.008 for PWV_{CA} and VWA_{AO}).

Finally, the association between PWV_{AO} and PWV_{CA} was statistically significant (Figure 4A) as well as the association between VWA_{AO} and VWA_{CA} (Figure 4B).

Moreover, in a forward selection model, VWA_{AO} was selected (p<0.0001) for prediction for PWV_{AO}, whereas VWA_{CA} was not independently associated (p=0.6) with PWV_{AO} after correction for VWA_{AO}. In addition, for predicting PWV_{CA}, VWA_{CA} (p<0.0001) was selected, whereas VWA_{AO} was not independently (p=0.8) associated with PWV_{CA}.

Figure 2-4. Linear regression analyses for the associations and the age-adjusted associations-between PWV and VWA. Values of VWA are plotted to a logarithmic scale.

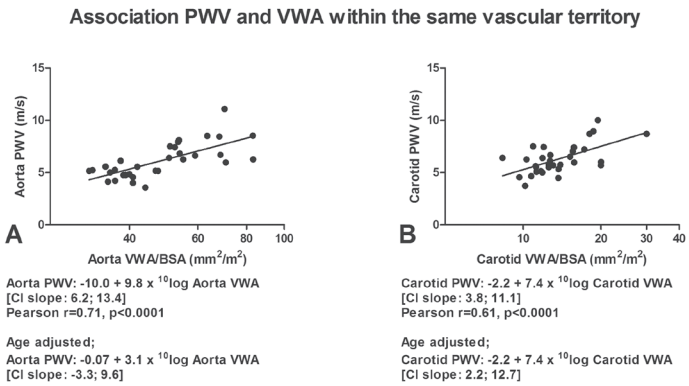

Figure 2A: PWV_{AO} and VWA_{AO} (i.e. within the same vascular territory). **Figure 2B**: PWV_{CA} and VWA_{CA} (i.e. within the same vascular territory).

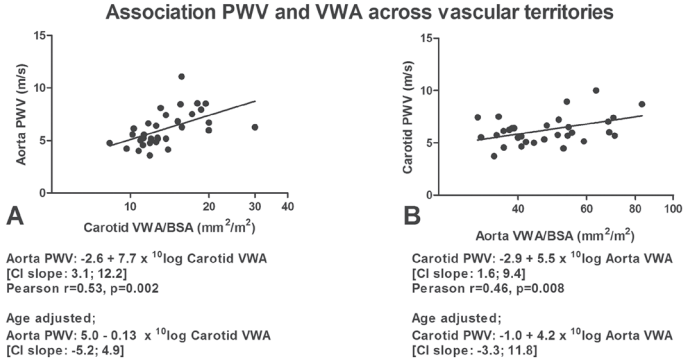

Figure 3A: PWV_{AO} and VWA_{CA} (i.e. across vascular territories). **Figure 3B**: PWV_{CA} and VWA_{AO} (i.e. across vascular territories).

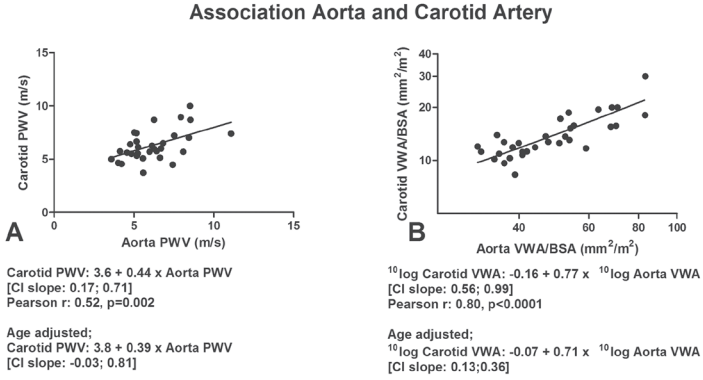

Figure 4A: PWV_{AO} and PWV_{CA}. **Figure 4B**: VWA_{AO} and VWA_{CA}.

Table 3: Correlation between vessel wall properties

	Aorta PWV	Carotid PWV	^{10}log Aorta VWA	^{10}log Carotid VWA
Aorta PWV	1	0.52 (0.002)	0.71 (<0.0001)	0.53 (0.002)
Carotid PWV	0.52 (0.002)	1	0.46 (0.008)	0.61 (p<0.0001)
^{10}log Aorta VWA	0.71 (<0.0001)	0.46 (0.008)	1	0.8 (<0.0001)
^{10}log Carotid VWA	0.53 (0.002)	0.61 (<0.0001)	0.8 (<0.0001)	1

Data are represented as Pearson correlation (p-value)
Abbreviations: PWV: pulse wave velocity, VWA: vessel wall area.

DISCUSSION

The current study demonstrated that morphologic and functional vessel wall properties in aorta and carotid artery are significantly associated. The main finding of our study is that this association was stronger within the same vascular territory, for both the aorta and the carotid artery, rather than across different vascular territories. To the best of our knowledge, our study is the first to report an evaluation of both VWA and PWV-assessment in the aorta as well as in the left carotid artery by using VE MRI.

Our findings highlight the potential of 3T MRI for non-invasive assessment of both PWV and VWA in the aorta and the carotid artery. Indeed, the assessment of arterial stiffness by PWV at *various* vascular territories to evaluate the predictive value for vascular events is of clinical interest (1,4,6).

Aortic stiffening is well-known to be associated with cardiovascular disease (1,12,19). However, recently it was suggested that the PWV-ratio between the aortic arch and the carotid artery may be an independent predictor for specific end-organ damage in the brain (4,6). With aging and the influence of atherosclerotic risk factors, stiffening of the aorta may be increased over stiffening of the carotid artery, potentially leading to the transmission of excessive pulsatile energy towards the brain microcirculation (3-5).

Previous studies almost exclusively used applanation tonometry and echo Doppler for arterial stiffness assessment (4,5,20,21). Both modalities can only provide an estimation of the global PWV in the whole aorta, due to the unavailability of appropriate acoustic windows to image the complete vascular tree, the inability of accurate determination of the wave propagation path length (7). MRI has several advantages over echo Doppler; it allows for precise measurement of this path length and direct sampling of aortic PWV and carotid arterial PWV over a longer trajectory (especially for the carotid artery) is possible, without any restriction regarding the choice of imaging plane.

Associations between PWV and VWA within the same vascular territory

Our study showed significant associations between PWV_{AO} and VWA_{AO} and between PWV_{CA} and VWA_{CA}. This coupling between wall morphology and function within the same vascular territory is in line with the concept of aortic stiffness described by the Moens-Korteweg equation, which describes a direct relation between local PWV and diameter, thickness and elastic properties of the vessel wall (1). Altered mechanical

properties of the vessel wall may influence the development of vessel wall thickening and/or presence of vessel wall thickening itself may increase arterial stiffness, or both mechanisms apply and may result in a self-perpetuating process (3,21). Interestingly, in the present study, the association between PWV and VWA within the aorta seemed more influenced by age than within the carotid artery. This finding is in line with a previous study describing that the aorta has a higher sensitivity to vascular aging, including incremental collagen content and calcification of the vessel wall media (22). Moreover, an arterial-specific age-relation of aortic and carotid arterial stiffness has been observed (5).

Associations between PWV and VWA across vascular territories

We also observed significant cross-link associations between PWV and VWA of the aorta and carotid artery. Our findings are in line with a previous study describing the association between aortic stiffness and increased carotid arterial intima-media thickness (IMT) (21). In atherosclerosis, gradual arterial changes are considered to be part of a diffuse systemic process, affecting different sites of the vascular tree. Therefore, associations between PWV and VWA across vascular territories are to be expected. However, for the aorta and the carotid artery, the association between PWV and VWA within the same vascular territory was stronger than the association between PWV and VWA across the vascular territories. This may suggest that sampling of IMT in the carotid artery might not be the most optimal measurement to assess the status of atherosclerosis in the aorta or in an even more remote vascular territory such as the peripheral arteries. Our finding is in line with a recent study by Brandts et al. (17), where in patients with hypertension, a stronger association was described between aortic PWV and aortic VWA than between aortic PWV and carotid VWA. In that study, PWV was only assessed for the aorta. Additionally, we present complete associations between PWV and VWA, in both the aorta as well as in the carotid artery. In our study, PWV_{CA} was significantly associated with both carotid artery VWA and with aorta VWA, but similar to the findings for the aorta, the strength of the association between PWV and VWA within the same vascular territory was stronger than across different vascular territories. Moreover, in forward selection models, only the site-specific VWA was selected for prediction of PWV. The stronger association between morphology and function within the same vascular territory as compared to the association across vascular territories is in line with the concept of arterial specific vascular aging.

Limitations

Our study has some limitations. First, it involves a cross-sectional design in a relatively small selective population of healthy volunteers. Follow-up studies are needed to further elucidate the associations between aortic and carotid arterial PWV and VWA in a large cohort of normal volunteers and in different patient populations. Moreover, for comparison purposes, sampling of VWA was standardized to a limited selected segment of 1.6 cm for the carotid artery and 2 cm for the aorta. Increasing the segment trajectory

length or adding segments at other parts of the aorta and carotid artery is of course feasible at the penalty of an increasing acquisition time.

Second, assessment of PWV_{CA} by VE MRI has not been validated against invasive pressure measurements, as was previously done for PWV_{AO} (9). However, the same imaging technique and image processing strategy were followed as for the well-validated PWV_{AO}-assessment.

Moreover, PWV-assessment using MRI is time-consuming and relatively expensive in comparison to echocardiography. However, previous studies using echocardiography only used carotid arterial IMT measurements as surrogate marker of generalized atherosclerosis, whereas MRI allows for site-specific sampling, since it is not restricted regarding the choice of imaging plane, i.e. measuring the aorta in patients with site-specific *subclinical* atherosclerosis in the aorta.

Conclusion

In conclusion, we have demonstrated that functional and morphologic vessel wall properties in aorta and carotid artery were significantly stronger associated when sampled within the same vascular territory rather than across different vascular territories, reflecting site-specific coupling of cross-sectional vessel wall area and function.

REFERENCES

1. Cavalcante JL, Lima JA, Redheuil A, Al-Mallah MH. Aortic stiffness current understanding and future directions. J Am Coll Cardiol 2011;57:1511-1522.
2. Lloyd-Jones D, Adams RJ, Brown TM et al. Heart disease and stroke statistics—2010 update: a report from the American Heart Association. Circulation 2010;121:e46-e215.
3. Lakatta EG, Levy D. Arterial and cardiac aging: major shareholders in cardiovascular disease enterprises: Part I: aging arteries: a "set up" for vascular disease. Circulation 2003;107:139-146.
4. Mitchell GF, van Buchem MA, Sigurdsson S et al. Arterial stiffness, pressure and flow pulsatility and brain structure and function: the Age, Gene/Environment Susceptibility—Reykjavik study. Brain 2011;134:3398-3407.
5. Mitchell GF. Effects of central arterial aging on the structure and function of the peripheral vasculature: implications for end-organ damage. J Appl Physiol 2008;105:1652-1660.
6. King KS, Chen KX, Hulsey KM et al. White matter hyperintensities: use of aortic arch pulse wave velocity to predict volume independent of other cardiovascular risk factors. Radiology 2013;267:709-717.
7. Corti R, Fuster V. Imaging of atherosclerosis: magnetic resonance imaging. Eur Heart J 2011;32:1709-1719.
8. Fayad ZA, Mani V, Fuster V. The time has come for clinical cardiovascular trials with plaque characterization as an endpoint. Eur Heart J 2012;33:160-161.
9. Grotenhuis HB, Westenberg JJ, Steendijk P et al. Validation and reproducibility of aortic pulse wave velocity as assessed with velocity-encoded MRI. J Magn Reson Imaging 2009;30:521-526.
10. Roes SD, Westenberg JJ, Doornbos J et al. Aortic vessel wall magnetic resonance imaging at 3.0 Tesla: a reproducibility study of respiratory navigator gated free-breathing 3D black blood magnetic resonance imaging. Magn Reson Med 2009;61:35-44.
11. Kroner ES, van der Geest RJ, Scholte AJ et al. Evaluation of sampling density on the accuracy of aortic pulse wave velocity from velocity-encoded MRI in patients with Marfan syndrome. J Magn Reson Imaging 2012;36:1470-1476.
12. Brandts A, van Elderen SG, Westenberg JJ et al. Association of aortic arch pulse wave velocity with left ventricular mass and lacunar brain infarcts in hypertensive patients: assessment with MR imaging. Radiology 2009;253:681-688.
13. Edelman RR, Chien D, Kim D. Fast selective black blood MR imaging. Radiology 1991;181:655-660.
14. Alizadeh DR, Doornbos J, Tamsma JT et al. Assessment of the carotid artery by MRI at 3T: a study on reproducibility. J Magn Reson Imaging 2007;25:1035-1043.
15. Westenberg JJ, de Roos A, Grotenhuis HB et al. Improved aortic pulse wave velocity assessment from multislice two-directional in-plane velocity-encoded magnetic resonance imaging. J Magn Reson Imaging 2010;32:1086-1094.
16. Adame IM, van der Geest RJ, Wasserman BA, Mohamed MA, Reiber JH, Lelieveldt BP. Automatic segmentation and plaque characterization in atherosclerotic carotid artery MR images. MAGMA 2004;16:227-234.
17. Brandts A, Westenberg JJ, van Elderen SG et al. Site-specific coupling between vascular wall thickness and function: an observational MRI study of vessel wall thickening and stiffening in hypertension. Invest Radiol 2013;48:86-91.
18. Mosteller RD. Simplified calculation of body-surface area. N Engl J Med 1987;317:1098.

19. van Elderen SG, Brandts A, Westenberg JJ et al. Aortic stiffness is associated with cardiac function and cerebral small vessel disease in patients with type 1 diabetes mellitus: assessment by magnetic resonance imaging. Eur Radiol 2010;20:1132-1138.
20. Mitchell JR, Schwartz CJ. Relationship between arterial disease in different sites. A study of the aorta and coronary, carotid, and iliac arteries. Br Med J 1962;1:1293-1301.
21. van Popele NM, Grobbee DE, Bots ML et al. Association between arterial stiffness and atherosclerosis: the Rotterdam Study. Stroke 2001;32:454-460.
22. Paini A, Boutouyrie P, Calvet D, Tropeano AI, Laloux B, Laurent S. Carotid and aortic stiffness: determinants of discrepancies. Hypertension 2006;47:371-37